

Curing $O(a)$ Errors in 3-D Lattice $SU(2) \times U(1)$ Higgs Theory

Guy D. Moore¹

*Princeton University
Joseph Henry Laboratories, PO Box 708
Princeton, NJ 08544, USA*

Abstract

We show how to make $O(a)$ corrections in the bare parameters of 3-D lattice $SU(2) \times U(1)$ Higgs theory which remove $O(a)$ errors in the match between the infrared behavior and the infrared behavior of the continuum theory. The corrections substantially improve the convergence of lattice data to a small a limit.

PACS numbers: 11.15.Ha, 11.15.Kc

Keywords: Dimensional reduction, Finite spacing effects, Electroweak phase transition, Baryogenesis

1 Introduction

It is believed that the baryon number of the universe may have originated at the electroweak phase transition. The details of the mechanism depend substantially on the details of the phase transition itself, so for several years there has been growing interest in a quantitative understanding of the electroweak phase transition. Ordinary perturbation theory [1] has proven useful only when the Higgs mass $m_H \ll m_W$ the W mass, and outside of this regime the only reliable methods are nonperturbative, such as lattice Monte-Carlo techniques.

The reason for the failure of perturbation theory was elucidated by the work of Farakos et. al. [2, 3, 4], who have shown how, to very good approximation, the thermodynamics of the standard model near the electroweak phase transition can be described using a three

¹e-mail: guymoore@puhep1.princeton.edu

dimensional path integral for purely bosonic $SU(2)\times U(1)$ Higgs theory. The theory is superrenormalizable, and hence its ultraviolet is well behaved, but its infrared is potentially nonperturbative, leading to the breakdown of perturbation theory as a tool for exploring the basically infrared physics of the phase transition. However, this same feature makes the numerical investigation of the nonperturbative physics particularly feasible; fine lattices are possible because the system is low dimensional, the couplings fall quickly with lattice spacing, and there is no need for the (numerically expensive) inclusion of fermionic degrees of freedom.

Several groups have conducted numerical experiments on the three dimensional system to study the phase transition [5, 6, 7, 8, 9, 10]. Each study used the Wilson action and the bare relations between lattice couplings and wave functions and the 3-D continuum parameters. In each case there were substantial linear in a (lattice spacing) errors which had to be removed by extrapolation over several values of a . The extrapolation process is numerically expensive because it demands very fine lattices, and if the extrapolation is large, as it is in several cases, one may wonder about its reliability. It would be better to have an analytic understanding of the origin of the linear in a corrections, which would make it possible to remove them. This paper presents such an analysis.

The $O(a)$ errors in measured infrared phenomena arise because the infrared theory is clothed by interactions with more ultraviolet modes, but the clothing differs between lattice and continuum theories, both because the most ultraviolet degrees of freedom are absent on the lattice, and because the ultraviolet lattice modes have incorrect dispersion relations and extra (lattice artefact) interactions. Since the dispersion relations and couplings of the lattice theory agree with those of the continuum theory in the infrared, the difference between clothing in the two theories is all ultraviolet, and therefore perturbatively computable. Also, since the origin of the difference is ultraviolet, it should be expressible as an operator expansion, and at the desired level of accuracy only the superrenormalizable terms are needed; these can be compensated for by a shift in the bare parameters of the theory.

The outline of the paper is as follows. In Section 2 we present the problem, establish notation, and give the results. Readers uninterested in the details of the calculation can then skip Section 3, which enumerates the required Feynman diagrams, presents the calculation of a few, and gives results for the others. The conclusion, Section 4, contains an example of using the improvement technique to reinterpret existing data. The first two appendices contain integrals, identities, and Feynman rules needed in Section 3, and the last presents the results for the abelian Higgs model, and for the standard model but including the adjoint scalar (A_0) fields.

2 Set-up and Results

The dimensional reduction program shows that the thermodynamics of the standard model are described up to small error by the partition function

$$Z = \int \mathcal{D}\Phi \mathcal{D}A_i \mathcal{D}B_i \exp(-\beta \int d^3x H), \quad (1)$$

$$H = \frac{1}{4g^2} \left(F_{ij}^a F_{ij}^a + \frac{1}{\tan^2 \Theta_W} f_{ij} f_{ij} \right) + (D_i \Phi)^\dagger (D_i \Phi) + m_H^2(\mu) \Phi^\dagger \Phi + \lambda (\Phi^\dagger \Phi)^2. \quad (2)$$

Here A_i and B_i are the gauge fields and F_{ij}^a and f_{ij} are the field strengths of the SU(2) and U(1) gauge groups respectively, and the couplings and wave function normalizations are determined with respect to physical measurables as discussed in [4]. Only m_H^2 depends on the ($\overline{\text{MS}}$) renormalization point μ .

The corresponding (Wilson) lattice action, in lattice units, is

$$Z = \int \mathcal{D}U \mathcal{D}u \mathcal{D}\Phi \exp(-\beta_L \sum_x H_L), \quad (3)$$

$$H_L = \sum_{i<j} (1 - \frac{1}{2} \text{Tr} P_{ij}) + \frac{1}{\tan^2 \Theta_W} \sum_{i<j} (1 - \text{Re } p_{ij}) \\ + \sum_i \left(\Phi_a^2(x) - \Phi_a(x) U_{iab}(x) u_{ibc}(x) \Phi_c(x+i) \right) + \frac{m_{HL}^2}{2} \Phi_a^2 + \frac{\lambda_L}{4} (\Phi_a^2)^2, \quad (4)$$

where Φ is treated as four independent real entries Φ_a , U and u are the SU(2) and U(1) link variables respectively, and P_{ij} and p_{ij} are the SU(2) and U(1) 1×1 plaquettes. The notation for Φ_a is equivalent to the common notation in which the Higgs field is written as a magnitude times an $SU(2)$ matrix, and each sum on a is replaced by $(1/2)\text{Tr}$.

The (naive) tree relations between the lattice parameters and the 3-D continuum ones are

$$\beta_L = \frac{4\beta}{g^2 a}, \quad (5)$$

$$\lambda_L = \frac{4\lambda}{g^2}, \quad (6)$$

$$\beta_L^2 \Phi_a^2 = \frac{8\Phi^\dagger \Phi}{g^2} = \frac{4\phi^2}{g^2}, \quad (7)$$

$$m_{HL}^2 = \frac{4\beta_L^2 m_H^2}{g^2}, \quad (8)$$

$$\tan^2 \Theta_W = \tan^2 \Theta_W. \quad (9)$$

All but Eq.(8) should hold in the continuum (small a or large β_L) limit, and this one does not because of the two powers of β_L on the righthand side; the Higgs mass does not scale with the lattice spacing in the same way as the wave functions and the scalar self-coupling, but needs to vanish quadratically, in lattice units, as the lattice spacing is made smaller. Hence, it receives linearly and logarithmically divergent corrections, which have been computed in [3, 11].

Note that, for any process which does not involve frequencies well to the infrared of the reciprocal lattice spacing, the lattice system is almost linear, with perurbation expansion coefficient β_L^{-1} . This is because each vertex contains a factor of β_L , and each propagator contains a β_L^{-1} , so for each loop there will be a β_L^{-1} . Hence the theory at the lattice scale becomes more perturbative linearly as the lattice spacing is reduced.

At nonzero a the lattice and continuum system cannot be made to agree perfectly. In particular the action used contains high dimension operators, which are gauge and cubic point group invariant and will therefore only contaminate the infrared theory at even powers of β_L^{-1} . But the disagreement in the infrared begins already at $O(\beta_L^{-1})$ because screening

$$\begin{aligned}
\text{Diagram: } \text{---} \bullet \text{---} &= \text{---} + \text{---} \bullet \text{---} \text{---} \bullet \text{---} \bullet \text{---} \bullet \text{---} \bullet \text{---} \\
\mathbf{G} &= \frac{Z^{-1}}{p^2 + m_H^2 - \delta m_H^2} + \frac{Z^{-1}}{p^2 + m_H^2 - \delta m_H^2} \pi \mathbf{G}
\end{aligned}$$

Figure 1: Relation between bare and clothed propagator at one loop.

by ultraviolet modes effectively modifies the infrared couplings and wave functions. Such effects can only arise from one loop diagrams, because β_L^{-1} is the expansion parameter of the perturbation theory at the lattice spacing scale. It is best to make $O(\beta_L^{-1})$ shifts from the tree relations given above to absorb the shifts due to screening (actually, due to the mismatch between the screening expected in the continuum theory and that realized in the lattice theory). Two loop effects will require $O(\beta_L^{-2})$ corrections, and at this level one should also remove the first set of tree level nonrenormalizable operators; but here we will only attempt to remove the $O(\beta_L^{-1})$ errors.

The most general form for the new bare action is

$$\begin{aligned}
H_L &= Z_A \sum_{i<j} (1 - \frac{1}{2} \text{Tr} P_{ij}) + \frac{Z_B}{\tan^2 \Theta_W} \sum_{i<j} (1 - \text{Re} p_{ij}) \\
&+ Z_\Phi \sum_i (\Phi_a^2(x) - \Phi_a(x) U_{iab}(x) u_{ibc}(x) \Phi_c(x+i)) \\
&+ Z_\Phi \frac{m_{HL}^2 - \delta m_{HL}^2}{2} \Phi_a^2 + Z_\Phi^2 \frac{\lambda_L - \delta \lambda_L}{4} (\Phi_a^2)^2.
\end{aligned} \tag{10}$$

The Φ^2 operator should also receive a multiplicative renormalization, so $Z_{OP} \Phi_a^2$ rather than Φ_a^2 should be converted to the continuum value using Eq. (7). In addition there is an additive renormalization of Φ_a^2 , but since this is common to both electroweak phases, it cancels from physically interesting questions involving the jump in the order parameter.

The values for the renormalization constants are determined by the requirement that they cause the values of infrared propagators and vertices, computed to one loop, to match between the continuum and lattice theories. For instance, in the continuum theory the value of the scalar propagator is $G(p^2) = 1/(p^2 + m_H^2 - \pi_{\Phi,C}(p^2))$, with $\pi_{\Phi,C}$ the continuum theory self-energy computed using the clothed vertices and propagators, expressed in lattice units. In the lattice theory the bare propagator is modified by Z_Φ^{-1} , so the clothed propagator is (see Figure 1)

$$G = \frac{Z_\Phi^{-1}}{p^2 + m_{HL}^2 - \delta m_{HL}^2} (1 + \pi_{\Phi,L} G), \tag{11}$$

and hence

$$(Z_\Phi - 1)p^2 + (Z_\phi - 1)m_{HL}^2 - Z_\Phi \delta m_{HL}^2 = \pi_{\Phi,L} - \pi_{\Phi,C}. \tag{12}$$

Hence one can determine δm_{HL}^2 and Z_Φ from the difference between the lattice and continuum self-energies at $O(p^0)$ and $O(p^2)$. The self-energies should be computed using clothed vertices and wave functions, which coincide (by hypothesis) in the infrared; so the difference will be ultraviolet dominated, and here the clothed vertices and wave functions can be replaced by bare ones (without Z and $\delta\lambda$ corrections) with an $O(\beta_L^{-1})$ error, which would be accounted for in a full two loop calculation and will only lead to an $O(\beta_L^{-2})$ error in Z_Φ , and can therefore be neglected². Similarly, the $(Z_\Phi - 1)m_{HL}^2$ can be dropped (m_{HL}^2 being $O(\beta_L^{-2})$), and the Z_Φ in front of δm_{HL}^2 can be set to 1.

Next, denoting the loop contribution to the amputated 1PI four point function at small (zero) external momentum as $-V_\lambda$ (the minus sign because the contribution from the scalar self-coupling is $-\lambda$), and again denoting the lattice and continuum values with L and C subscripts respectively, one demands that

$$(\lambda_L - \delta\lambda_L)Z_\Phi^2 + V_{\lambda,L} = \lambda_L + V_{\lambda,C}, \quad (13)$$

and hence

$$\delta\lambda_L = V_{\lambda,L} - V_{\lambda,C} + 2\lambda(Z_\Phi - 1). \quad (14)$$

Again, the V_λ should be computed using the naive bare propagators and vertices because the difference will be ultraviolet dominated.

To find Z_A and Z_B one must compute not only the gauge field self-energy corrections π_A and π_B , but also the corrections to the gauge-scalar vertex, which we will denote as V_A, V_B . (It does not matter which vertex is considered, by gauge invariance; we choose the scalar vertex because it is the easiest to compute.) Z_A should be chosen so that the complete effect of a gauge particle propagating between two lines, say two scalar lines, is the same between the lattice and continuum theories, see Figure 2. The strength of the vertex at each end of the propagator is multiplied by $Z_\Phi + V_{A,L}$ in the lattice theory and $1 + V_{A,C}$ in the continuum theory; the Z_Φ factor arises because its appearance in the action modifies both the wave function and the coupling to the gauge field. The modification of the propagator is similar to that for the scalar, and we find that to match the full modification (a vertex at each end and a propagator in the middle) we must choose Z_A such that

$$\frac{(Z_\Phi + V_{A,L})^2}{Z_A p^2 - \pi_{A,L}} = \frac{1 + V_{A,C}}{p^2 - \pi_{A,C}}, \quad (15)$$

or, at leading order in β_L^{-1} ,

$$Z_A - 1 = 2(Z_\Phi - 1) + 2(V_{A,L} - V_{A,C}) + \frac{\pi_{A,L} - \pi_{A,C}}{p^2}. \quad (16)$$

The equation for Z_B is analogous, and in this case the vertex and Higgs wave function contributions will cancel.

²The one loop calculation envisioned here will only be able to reproduce the linearly divergent counterterm for the mass squared, so the determination of this quantity is not as good as the wave functions and couplings. However, this only degrades our ability to study the phase transition temperature, not its strength. Since the strength of the phase transition is much more interesting from the point of view of baryogenesis, ignorance of the phase transition temperature is not really a problem

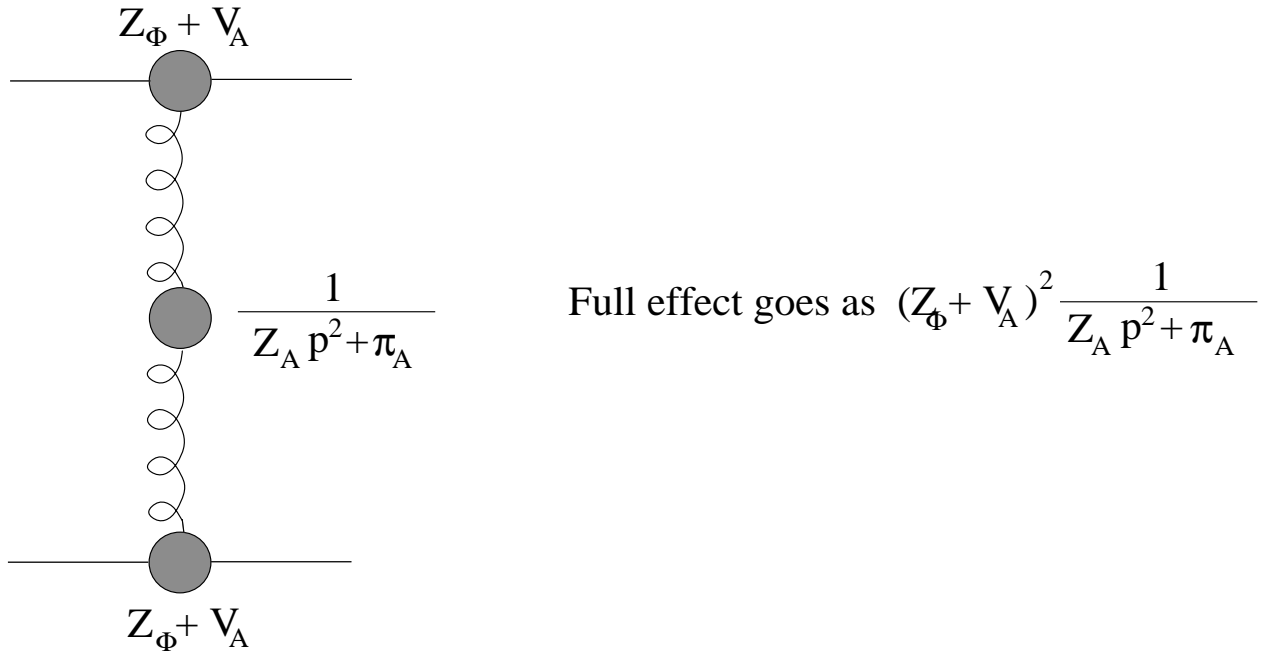


Figure 2: The full influence of a gauge particle propagating between two lines depends on the vertex and propagator renormalizations. Here and throughout SU(2) lines will be curly and U(1) lines will be wiggly.

The Φ^2 operator multiplicatively renormalizes due to the diagrams shown in Figure 8. If the sum of the contributions of the diagrams there, at small (zero) external momentum, are denoted by $L_{\Phi,L}$, and the continuum contribution is $L_{\Phi,C}$, then the renormalization of the Φ^2 operator is

$$Z_{OP} = 1 - (L_{\Phi,L} - L_{\Phi,C}). \quad (17)$$

Notice again that the L should be computed with clothed propagators, vertices, and operator insertions. Again, at the correct value of Z_{OP} the infrared definition of the operator insertions will coincide, so there is no divergent contribution to the difference arising from the infrared; the difference is UV dominated and can be computed, at the desired level of accuracy, with the bare vertices and propagators.

It is possible to scale Φ by a constant κ without changing the physics, provided one multiplies Z_Φ by κ^{-2} and Z_{OP} by κ^{-2} . Only the combination $Z_\Phi Z_{OP}^{-1}$ must be meaningful and gauge invariant. It is convenient to perform such a scaling of Φ to set Z_{OP} to 1, in which case one should add $(L_{\Phi,L} - L_{\Phi,C})$ to Z_Φ at the very end of the calculation.

The diagrams needed for the renormalization are presented in the next section, and their values are tabulated there. All but two are performed in lattice Lorentz gauge with a general gauge parameter, to check gauge parameter independence; the exceptions are the gauge field self-energy diagrams with all gauge vertices, which are only performed in Feynman gauge; so we have not yet checked the gauge invariance of Z_A . The results of the calculation are

$$Z_A - 1 = \beta_L^{-1} \left(21 \frac{\xi}{4\pi} + \frac{11}{12} \frac{\Sigma}{4\pi} + \frac{1}{3} \right), \quad (18)$$

$$Z_B - 1 = \beta_L^{-1} \tan^2 \Theta_W \left(-\frac{\xi}{4\pi} + \frac{1}{4} \frac{\Sigma}{4\pi} + \frac{1}{3} \right), \quad (19)$$

$$Z_\Phi Z_{OP}^{-1} - 1 = \beta_L^{-1} \left((9 + 3 \tan^2 \Theta_W - 6\lambda) \frac{\xi}{4\pi} + \frac{3 + \tan^2 \Theta_W}{6} \frac{\Sigma}{4\pi} \right), \quad (20)$$

$$\delta m_{HL}^2 = \beta_L^{-1} (6 + 2 \tan^2 \Theta_W + 6\lambda_L) \frac{\Sigma}{4\pi}, \quad (21)$$

$$\delta \lambda_L = \beta_L^{-1} \left((-12\lambda_L^2 - 4 - 2(1 + \tan^2 \Theta_W)^2 + 6\lambda_L(3 + \tan^2 \Theta_W)) \frac{\xi}{4\pi} + \frac{3 + \tan^2 \Theta_W}{3} \lambda_L \frac{\Sigma}{4\pi} \right). \quad (22)$$

The constants $\Sigma = 3.175911536$ and $\xi = 0.152859325$ have the same meaning as in [3], and arise from integrals presented in Appendix A. If one is interested in the theory without the U(1) gauge group, set $\tan^2 \Theta_W = 0$ and disregard Z_B . Equations (18)–(22) are the main result of this paper.

By applying these corrections to the Hamiltonian of a lattice simulation one should be able to remove all $O(a)$ errors. If one already has numerical data, then the $O(a)$ errors can be removed by re-interpreting the meaning of the answers. In the case of SU(2) Higgs theory alone, equating

$$\beta_{naive} \left(\sum 1 - \frac{1}{2} \text{Tr} P_{ij} + \frac{1}{2} \Phi_{a,naive} D_{Latt,ab}^2 \Phi_{b,naive} + \frac{m_{HL}^2 - \delta m_{HL}^2}{2} \Phi_{naive}^2 + \frac{\lambda_{L,naive}}{4} (\Phi_{naive}^2)^2 \right) \quad (23)$$

with

$$\beta_{imp} \left(Z_A \sum 1 - \frac{1}{2} \text{Tr} P_{ij} + \frac{1}{2} Z_\Phi \Phi_{a,imp} D_{Latt,ab}^2 \Phi_{b,imp} + Z_\Phi \frac{m_{HL}^2 - \delta m_{HL}^2}{2} \Phi_{imp}^2 + Z_\Phi^2 \frac{\lambda_{L,imp} - \delta \lambda_L}{4} (\Phi_{imp}^2)^2 \right), \quad (24)$$

one finds as matching conditions

$$\beta_{imp} = Z_A^{-1} \beta_{naive}, \quad (25)$$

$$\lambda_{L,imp} = Z_A^{-1} \lambda_{L,naive} + \delta \lambda_L, \quad (26)$$

$$\beta_{imp}^2 Z_{OP} \Phi_{imp}^2 = Z_\Phi^{-1} Z_{OP} Z_A^{-1} \beta_{naive}^2 \Phi_{naive}^2. \quad (27)$$

One should re-interpret at what temperature the simulation was conducted, what input value of λ_L was used, and what the result for $\beta_L^2 \Phi^2$ was. Note both that the value of $\lambda_{L,imp}$ is smaller than the value of $\lambda_{L,naive}$ and that the rescaling of $\beta_L^2 \Phi^2$ reduces its value. Both lead to an overestimate (before correction) of the strength of the phase transition, the first because the phase transition is stronger at smaller λ and the second because the real jump in the order parameter is smaller than that using naive conversions. The error in λ is the most problematic, because at small values of λ the strength of the phase transition is strongly λ dependent (one loop perturbation theory, which applies here, says the jump in Φ^2 should

go as λ^{-2}), and at larger values of λ the properties of the phase transition may change qualitatively as one changes λ . Note also that $Z_A - 1 \simeq 0.82\beta_L^{-1}$ is quite large, and so are corrections where Z_A appears.

One can get a rough understanding of the magnitudes of Z_A , Z_B , Z_Φ , and δm_{HL}^2 by considering the tadpole correction scheme of Lepage and Mackenzie [12]. Based on a mean field theory argument, they propose that the dominant loop contributions at every order can be absorbed by making an “educated guess” for the constants Z_A , etc, as follows: compute the mean value of the trace of an elementary plaquette, and call it U (or u for the U(1) plaquette). Then guess that every term in the action which contains a link should be multiplied by $U^{-1/4}$ (with the value of U found after the correction has been applied). Hence, Z_A should roughly equal U^{-1} , Z_Φ should roughly equal $U^{-1/4}u^{-1/4}$, Z_B should roughly equal u^{-1} , and δm_{HL}^2 should be about $6(U^{-1/4}u^{-1/4} - 1)$ (because the hopping term in the Higgs wave function gets corrected, but not the local term). It is quite easy to compute at one loop that $U = 1 - \beta_L^{-1}$ and $u = 1 - \tan^2 \Theta_W \beta_L^{-1}/3$. (This is just the approximation that the average energy in the plaquette term in the Hamiltonian obeys equipartition.) Hence, one guesses that, at lowest order in β_L ,

$$\beta_L(Z_A - 1) \simeq 1, \quad (28)$$

$$\beta_L(Z_B - 1) \simeq \frac{\tan^2 \theta_W}{3}, \quad (29)$$

$$\beta_L(Z_\Phi Z_{OP}^{-1} - 1) \simeq \frac{3 + \tan^2 \Theta_W}{12}, \quad (30)$$

$$\beta_L \delta m_{HL}^2 \simeq \frac{3 + \tan^2 \Theta_W}{2}. \quad (31)$$

In fact, at $\lambda_L = 0$, the numerical values of the corrections are

$$\beta_L(Z_A - 1) = 0.82, \quad (32)$$

$$\beta_L(Z_B - 1) = 0.384 \tan^2 \Theta_W, \quad (33)$$

$$\beta_L(Z_\Phi Z_{OP}^{-1} - 1) = 0.0786(3 + \tan^2 \Theta_W), \quad (34)$$

$$\beta_L \delta m_{HL}^2 = 0.505(3 + \tan^2 \Theta_W), \quad (35)$$

which are all quite close.

The tadpole improvement value for the correction to the scalar self-coupling is that it should only change due to the wave function correction. This misses the corrections at even powers of λ_L (though these are all suppressed by the rather small number $\xi/(4\pi)$). These corrections are important when λ_L is fairly small, because results are very λ_L sensitive in this regime. This illustrates a limitation of the tadpole improvement scheme in a theory with non-gauge couplings.

3 Details of the calculation

Here we will present the calculations of the vertices and self-energies needed in the last section in more detail. To illustrate what is involved in the calculation we will present the full details of the contribution of loops involving gauge particles to the scalar self-energy and

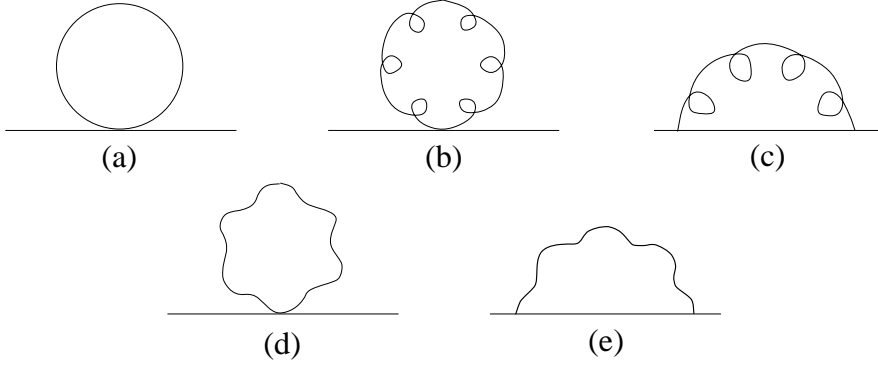


Figure 3: Diagrams contributing to the Higgs boson self-energy. The curly line refers to the SU(2) gauge particle, the wiggly line to the U(1) gauge particle, and the solid line to the scalar.

of scalar loops to the gauge field self-energy. For all other diagrams we will simply present results.

The diagrams contributing to the Higgs self-energy are presented in Figure 3. Diagram (a) is computed already in [3]. It is straightforward and leads to an $O(p^0)$ contribution to the difference in self-energies of

$$\pi_{\Phi,L} - \pi_{\Phi,C} = \beta_L^{-1} \left(-6\lambda_L \frac{\Sigma}{4\pi} \right) \quad \text{from (a)}. \quad (36)$$

Diagram (b) vanishes in the $\overline{\text{MS}}$ regulated continuum theory, so its contribution to the difference of self-energies in Landau gauge is

$$-\frac{3}{\beta_L} \int_{[-\pi,\pi]^3} \frac{d^3k}{(2\pi)^3} \frac{\delta_{ij} \left(\delta_{ij} - \frac{\tilde{k}_i \tilde{k}_j}{\tilde{k}^2} \right)}{\tilde{k}^2} \cos p_i, \quad (37)$$

where here and throughout p is the momentum of the line, $\tilde{k}_i = 2 \sin(k_i/2)$, and $\tilde{k}^2 = \sum_{i=1,2,3} \tilde{k}_i^2$. The factor of 3 is a group factor.

To make expressions more concise, the factor $d^3k/(2\pi)^3$ will henceforth be implied in every integral, continuum or lattice.

At small p , which is the interesting regime, $\cos(p_i) \simeq 1 - p_i^2/2$, and the contribution from diagram (b) becomes

$$\frac{-3}{\beta_L} \int_{[-\pi,\pi]^3} \left(\frac{2}{\tilde{k}^2} - \sum_i \frac{p_i^2}{2} \frac{\tilde{k}^2 - \tilde{k}_i^2}{(\tilde{k}^2)^2} \right). \quad (38)$$

The integral of $\tilde{k}_i^2/(\tilde{k}^2)^2$ is just 1/3 the integral of $1/\tilde{k}^2$ by cubic invariance, so the contribution of the diagram is

$$\pi_{\Phi,L} - \pi_{\Phi,C} = \beta_L^{-1} (-6 + p^2) \frac{\Sigma}{4\pi} \quad \text{from (b)}. \quad (39)$$

The contribution of (d) differs only in counting factors; the 3 is replaced with $\tan^2 \Theta_W$, which arises from the U(1) propagator.

In Landau gauge, diagram (c) on the lattice contributes

$$\pi_{\Phi,L} \text{ from } (c) = \frac{3}{\beta_L} \int_{[-\pi,\pi]^3} \frac{(2\widetilde{p}-k)_i(2\widetilde{p}-k)_j \left(\delta_{ij} - \frac{\widetilde{k}_i\widetilde{k}_j}{\widetilde{k}^2} \right)}{\widetilde{k}^2(p-k)^2}. \quad (40)$$

The continuum contribution is

$$\pi_{\Phi,C} \text{ from } (c) = \frac{3}{\beta_L} \int_{\mathfrak{R}^3} \frac{(2p-k)_i(2p-k)_j \left(\delta_{ij} - \frac{k_ik_j}{k^2} \right)}{k^2(p-k)^2}. \quad (41)$$

Each numerator vanishes at $p=0$, so to extract the $O(p^2)$ behavior we need only expand the numerator to $O(p^2)$ and use the denominator at $p=0$. (Each contribution is then separately infrared divergent, but the infrared divergences match and do not matter to the difference.) Since

$$(2\widetilde{p}-k)_i = 2 \sin(p_i - k_i/2) = -\widetilde{k}_i \cos(p_i) + 2\widetilde{p}_i \cos(k_i/2), \quad (42)$$

and \widetilde{k}_i annihilates against the gauge propagator (only because we are in Landau gauge), the contributions simplify at small p to

$$\begin{aligned} \pi_{\Phi,L} - \pi_{\Phi,C} \text{ from } (c) &= \frac{3}{\beta_L} \sum_{ij} 4p_i p_j \left(\int_{[-\pi,\pi]^3} \frac{\cos(k_i/2) \cos(k_j/2) (\delta_{ij} - \widetilde{k}_i\widetilde{k}_j/\widetilde{k}^2)}{(\widetilde{k}^2)^2} - \right. \\ &\quad \left. \int_{\mathfrak{R}^3} \frac{\delta_{ij} - k_ik_j/k^2}{k^4} \right). \end{aligned} \quad (43)$$

Each integral vanishes when $i \neq j$. When $i = j$, one may use $\cos^2(k_i/2) = 1 - \widetilde{k}_i^2/4$ and cubic invariance to reorganize the contribution as

$$\pi_{\Phi,L} - \pi_{\Phi,C} \text{ from } (c) = \frac{3p^2}{\beta_L} \left[\frac{8}{3} \left(\int_{[-\pi,\pi]^3} \frac{1}{(\widetilde{k}^2)^2} - \int_{\mathfrak{R}^3} \frac{1}{k^4} \right) - \frac{1}{3} \int_{[-\pi,\pi]^3} \frac{1}{\widetilde{k}^2} + \int_{[-\pi,\pi]^3} \frac{\widetilde{k}_1^4}{(\widetilde{k}^2)^3} \right]. \quad (44)$$

The first two integral expressions here are the constants $\xi/4\pi$ and $\Sigma/4\pi$. The last is related to these constants by an identity, Eq. (104). The result is

$$\pi_{\Phi,L} - \pi_{\Phi,C} \text{ from } (c) = \frac{3p^2}{\beta_L} \left(3 \frac{\xi}{4\pi} - \frac{1}{6} \frac{\Sigma}{4\pi} \right) \quad (45)$$

in Landau gauge. To get the contribution from diagram (e), replace the group factor, 3, with $\tan^2 \Theta_W$.

In this gauge, the numerical value of the contribution to the wave function renormalization from diagram (c) is $-0.017/\beta_L$, while the contribution from the ‘‘tadpole’’ diagram (b) is $+0.253/\beta_L$. The tadpole contribution is much bigger, even though diagram (b) vanishes in the continuum theory and would not naively be expected to contribute to the wave function renormalization at all. The contribution of this diagram almost exactly equals the expectation of the ‘‘tadpole improvement’’ argument.

For a general gauge parameter, where the gauge propagator becomes

$$\frac{\delta_{ij} + (\alpha - 1) \frac{\widetilde{k}_i\widetilde{k}_j}{\widetilde{k}^2}}{\widetilde{k}^2}, \quad (46)$$

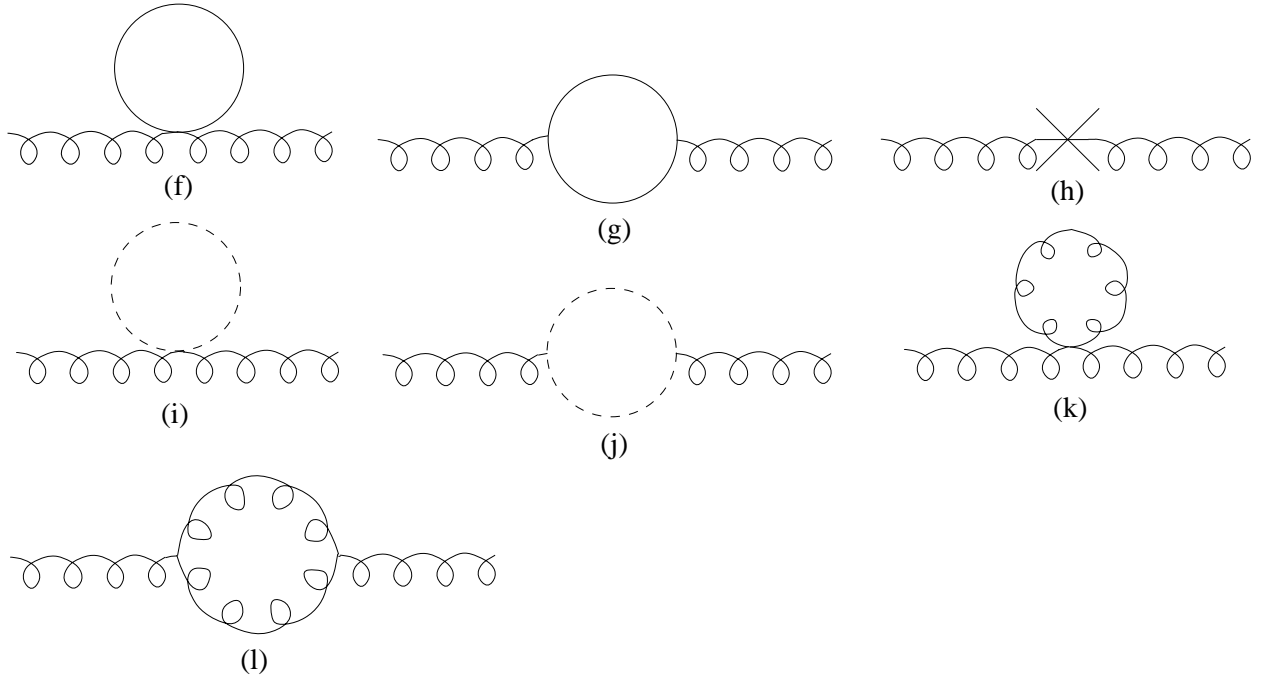


Figure 4: Contributions to the SU(2) gauge particle self-energy π_A . The curly line is the gauge particle, the solid line is the scalar, and the dotted line is the ghost.

the contribution from (b) changes by $\alpha(\Sigma/4\pi)(-3 + p^2/2)$, and the contribution from (c) changes by $-\alpha(\Sigma/4\pi)(-3 + p^2/2) - 3\alpha p^2 \xi/4\pi$. The mass squared correction is not gauge parameter dependent, but the wave function correction is. This will be canceled by a similar gauge parameter dependence in Z_{OP} .

New complications arise in computing the gauge particle self-energy. The value of the self-energy must be transverse and rotationally invariant, and it must approach zero at $p \rightarrow 0$; but individual diagrams need not separately satisfy these requirements. It is a nontrivial check on the calculation if they do, and on the lattice that check will involve the use of identities, which are intimately related to gauge invariance. To illustrate some of these issues we will present the calculation of the self-energy corrections from scalar loops. Two diagrams contribute, diagrams (f) and (g) in Figure 4. The contribution of (f), which vanishes in the $\overline{\text{MS}}$ renormalized continuum theory, is

$$\pi_{A,L} \text{ from } (f) = -\frac{2}{\beta_L} \delta_{AB} \delta_{ij} \int_{[-\pi, \pi]^3} \frac{\cos k_i}{\tilde{k}^2}, \quad (47)$$

where the 2 arises from the trace over the fundamental representation (in the standard continuum notation it would be 1/2, but here the coupling involves the Pauli matrix τ rather than $\tau/2$), and the δ_{AB} is in group space. Using $\cos k_i = 1 - \tilde{k}_i^2/2$ and cubic invariance, we perform the integrals and get

$$\pi_{A,L} \text{ from } (f) = -\frac{2}{\beta_L} \delta_{AB} \delta_{ij} \left(\frac{\Sigma}{4\pi} - \frac{1}{6} \right). \quad (48)$$

This does not vanish as $p \rightarrow 0$, and in fact does not depend on p at all. It is also independent of the gauge parameter α , because no gauge propagators appear in the loop.

Diagram (g) contributes

$$\pi_{A,L} \text{ from } (g) = \frac{2}{\beta_L} \delta_{AB} \frac{1}{2} \int_{[-\pi,\pi]^3} \frac{(\widetilde{2k})_i (\widetilde{2k})_j}{(k - p/2)^2 (k + p/2)^2} \quad (49)$$

in the lattice regulation and

$$\pi_{A,C} \text{ from } (g) = \frac{2}{\beta_L} \delta_{AB} \frac{1}{2} \int_{\mathbb{R}^3} \frac{2k_i 2k_j}{(k - p/2)^2 (k + p/2)^2} - \text{UV divergence} \quad (50)$$

in the continuum. The “−UV divergence” subtracts the value at $p = 0$. Hence the $O(p^0)$ contribution is just the lattice value, which is (using $(\widetilde{2k})_i = 2\tilde{k}_i \cos(k_i/2)$)

$$\frac{\delta_{AB}}{\beta_L} \int_{[-\pi,\pi]^3} \frac{4\tilde{k}_i \tilde{k}_j \cos(k_i/2) \cos(k_j/2)}{(\tilde{k}^2)^2} = \frac{\delta_{AB} \delta_{ij}}{\beta_L} \int_{[-\pi,\pi]^3} \frac{4\tilde{k}_1^2 - \tilde{k}_1^4}{(\tilde{k}^2)^2}. \quad (51)$$

The integral involving \tilde{k}_1^2 can be performed using cubic invariance and gives $(4/3)(\Sigma/4\pi)$, but it is not immediately obvious how to perform the other integral, or that its value will correctly cancel the other $O(p^0)$ parts. The integral is solved using the identity, Eq. (107), which was derived from the invariance of $\int_{[-\pi,\pi]^3} \ln(\tilde{k}^2)$ on shifting k_1 (which can be compensated for by a shift in the integration range). It does in fact cancel the other $O(a^0)$ parts arising from scalar loops.

To understand why, note that all 1 loop contributions to the gauge action from scalar loops can be computed by performing the integral over the Higgs fields in the Gaussian approximation (ie neglecting λ_L); the scalar loop contribution is $(-1/2)\text{Tr} \ln(-D^2 + m^2)$. This can then be expanded about $\text{Tr} \ln -\partial^2 + m^2 = \int_{[-\pi,\pi]^3} \ln(\tilde{k}^2 + m^2)$. The required identity came from shifting the integration variable in exactly this integral (at $m^2 = 0$), which is of course the same as applying a spatially nonvarying gauge field. In fact, Eq. (106) contains precisely the integrals in Eqs. (47) and (51) which contribute at $O(p^0)$.

Expanding the contribution from diagram (g) to $O(p^2)$ one finds, from Eq. (49),

$$\frac{\delta_{AB}}{\beta_L} \int_{[-\pi,\pi]^3} \frac{4\tilde{k}_i \tilde{k}_j \cos(k_i/2) \cos(k_j/2)}{(\tilde{k}^2)^2} \left[\sum_l \frac{p_l^2}{2\tilde{k}^2} \left(\frac{1}{2} \tilde{k}_l^2 - 1 \right) + \sum_{lm} p_l p_m \frac{\tilde{k}_l \tilde{k}_m \cos(k_l/2) \cos(k_m/2)}{(\tilde{k}^2)^2} \right]. \quad (52)$$

The corresponding continuum contribution is

$$\frac{\delta_{AB}}{\beta_L} \int_{\mathbb{R}^3} \frac{4k_i k_j}{k^4} \left[-\frac{p^2}{2k^2} + \frac{(p \cdot k)^2}{k^4} \right], \quad (53)$$

which removes the infrared divergence of the lattice version. The difference between the lattice and continuum expressions must be of form

$$\frac{\delta_{AB}}{\beta_L} (A \delta_{ij} p^2 + B p_i p_j + C \delta_{ij} p_i^2), \quad (54)$$

simply from cubic invariance. We expect that the answer will be rotationally invariant and transverse, $B = -A$ and $C = 0$, because all gauge invariant, cubic invariant, dimension 4 operators are; and this will constitute a check on the calculation. The p_1^2 contribution when $i = j = 1$ is

$$A + B + C = 4 \int_{[-\pi, \pi]^3} \frac{\tilde{k}_1^2(1 - \tilde{k}_1^2/4)}{(\tilde{k}^2)^2} \left(\frac{\tilde{k}_1^2 - 2}{4\tilde{k}^2} + \frac{\tilde{k}_1^2(1 - \tilde{k}_1^2/4)}{(\tilde{k}^2)^2} \right) - \text{IR divergence}, \quad (55)$$

which can be evaluated using Eq. (109) and Eq. (114) in Appendix A; it vanishes. One can find A from the p_2^2 contribution when $i = j = 1$; it equals

$$A = 4 \int_{[-\pi, \pi]^3} \frac{\tilde{k}_1^2(1 - \tilde{k}_1^2/4)}{(\tilde{k}^2)^2} \left(\frac{\tilde{k}_2^2 - 2}{4\tilde{k}^2} + \frac{\tilde{k}_2^2(1 - \tilde{k}_2^2/4)}{(\tilde{k}^2)^2} \right) - \text{IR divergence}, \quad (56)$$

which can be evaluated using Eq. (110) and Eq. (115), and equals

$$A = \frac{1}{4} \frac{\Sigma}{4\pi} - \frac{\xi}{4\pi}. \quad (57)$$

To evaluate B one takes the $p_1 p_2$ part when $i = 1$ and $j = 2$, which is

$$B = 4 \int_{[-\pi, \pi]^3} \frac{\tilde{k}_1^2 \tilde{k}_2^2 (1 - \tilde{k}_1^2/4)(1 - \tilde{k}_2^2/4)}{(\tilde{k}^2)^4} - \text{IR divergence} = -A, \quad (58)$$

evaluating it with the same equations. Hence $C = 0$ and the result is indeed rotationally invariant and transverse.

There are no new techniques involved in the remaining integrals, so we will simply tabulate all of the results here.

Five diagrams, (a) through (e) of Figure 3, contribute to the Higgs self-energy. They are evaluated above, and equal

$$\beta_L(\pi_{\Phi, L} - \pi_{\Phi, C}) = -6\lambda \frac{\Sigma}{4\pi} \text{ from (a)} + \quad (59)$$

$$(-6 - 3\alpha) \frac{\Sigma}{4\pi} + p^2 \left(1 + \frac{\alpha}{2}\right) \frac{\Sigma}{4\pi} \text{ from (b)} + \quad (60)$$

$$3\alpha \frac{\Sigma}{4\pi} + p^2 \left(\left(-\frac{1}{2} - \frac{\alpha}{2}\right) \frac{\Sigma}{4\pi} + (9 - 3\alpha) \frac{\xi}{4\pi} \right) \text{ from (c)} + \quad (61)$$

$$\left[(-2 - \alpha) \frac{\Sigma}{4\pi} + p^2 \left(\frac{1}{3} + \frac{\alpha}{6} \right) \frac{\Sigma}{4\pi} \right] \tan^2 \Theta_W \text{ from (d)} + \quad (62)$$

$$\left[\alpha \frac{\Sigma}{4\pi} + p^2 \left(\left(-\frac{1}{6} - \frac{\alpha}{6}\right) \frac{\Sigma}{4\pi} + (3 - \alpha) \frac{\xi}{4\pi} \right) \right] \tan^2 \Theta_W \text{ from (e)}. \quad (63)$$

Seven diagrams, (f) through (l) of Figure 4, contribute to the SU(2) field self-energy. In Feynman ($\alpha = 1$) gauge, they contribute (δ_{AB} understood)

$$\beta_L(\pi_{A, L} - \pi_{A, C}) = \delta_{ij} \left(-2 \frac{\Sigma}{4\pi} + \frac{1}{3} \right) \text{ from (f)} + \quad (64)$$

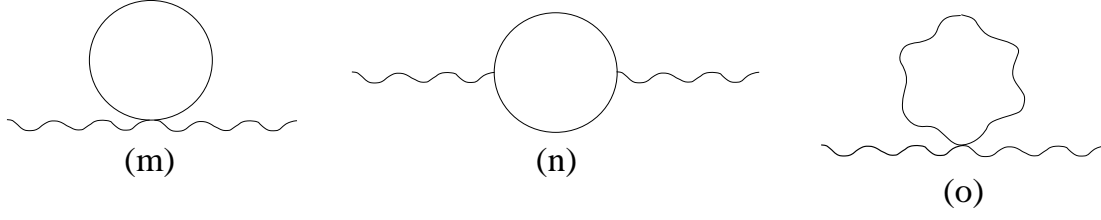


Figure 5: Contributions to the U(1) particle self-energy. The wiggly lines are the U(1) gauge particle, and the straight lines are the scalars. Diagram (o) only exists in the lattice theory.

$$\delta_{ij} \left(2 \frac{\Sigma}{4\pi} - \frac{1}{3} \right) + (\delta_{ij} p^2 - p_i p_j) \left(\frac{1}{4} \frac{\Sigma}{4\pi} - \frac{\xi}{4\pi} \right) \text{ from } (g) \quad + \quad (65)$$

$$\frac{-2}{3} \delta_{ij} \quad \text{from } (h) \quad + \quad (66)$$

$$\frac{-4}{9} \delta_{ij} \quad \text{from } (i) \quad + \quad (67)$$

$$\delta_{ij} \left(-4 \frac{\Sigma}{4\pi} + \frac{2}{3} \right) + \delta_{ij} p^2 \left(-\frac{1}{2} \frac{\Sigma}{4\pi} + 2 \frac{\xi}{4\pi} \right) + p_i p_j \frac{1}{2} \frac{\Sigma}{4\pi} \quad \text{from } (j) \quad (68)$$

$$\delta_{ij} \left(-16 \frac{\Sigma}{4\pi} + \frac{28}{9} \right) + \delta_{ij} p^2 \left(\frac{14}{3} \frac{\Sigma}{4\pi} \right) +$$

$$p_i p_j \left(-\frac{8}{3} \frac{\Sigma}{4\pi} - \frac{1}{3} \right) + \delta_{ij} p_i^2 \left(-2 \frac{\Sigma}{4\pi} + \frac{1}{3} \right) \quad \text{from } (k) \quad + \quad (69)$$

$$\delta_{ij} \left(20 \frac{\Sigma}{4\pi} - \frac{4}{3} \right) + \delta_{ij} p^2 \left(10 \frac{\xi}{4\pi} - \frac{23}{6} \frac{\Sigma}{4\pi} + \frac{1}{3} \right) +$$

$$p_i p_j \left(-12 \frac{\xi}{4\pi} + \frac{11}{6} \frac{\Sigma}{4\pi} \right) + \delta_{ij} p_i^2 \left(2 \frac{\Sigma}{4\pi} - \frac{1}{3} \right) \quad \text{from } (l). \quad (70)$$

Only the last two are gauge parameter dependent. The total is rotationally invariant, transverse, and free of $O(p^0)$ contributions.

Only three diagrams, (m) through (o) in Figure 5, contribute to π_B . The scalars have the same value as for the SU(2) self-energy, because although the SU(2) contribution is enhanced by a group factor of 2, the SU(2) doublet contains 2 fields which are charged under U(1). The result is

$$\frac{\beta_L}{\tan^2 \Theta_W} (\pi_{B,L} - \pi_{B,C}) = \delta_{ij} \left(-2 \frac{\Sigma}{4\pi} + \frac{1}{3} \right) \quad \text{from } (m) \quad + \quad (71)$$

$$\delta_{ij} \left(2 \frac{\Sigma}{4\pi} - \frac{1}{3} \right) + (\delta_{ij} p^2 - p_i p_j) \times$$

$$\left(\frac{1}{4} \frac{\Sigma}{4\pi} - \frac{\xi}{4\pi} \right) \quad \text{from } (n) \quad + \quad (72)$$

$$\frac{1}{3} (\delta_{ij} p^2 - p_i p_j) \quad \text{from } (o) \quad (73)$$

The factor of $\tan^2 \Theta_W$ arises as follows. Each B field propagator contributes a $\tan^2 \Theta_W$, and there is 1 more propagator when a self-energy insertion occurs than when none occurs; in the

case of diagram (o), there are two extra propagators, but the vertex contributes $\tan^{-2} \Theta_W$. Although this diagram does not exist in the continuum theory, it completely dominates the contribution to the self-energy. It arises from the compact nature of the gauge action, and its value is given *exactly* by the tadpole improvement technique at one loop.

Some 12 diagrams contribute to the scalar four point vertex, in a general gauge. All but 4 of these vanish in Landau gauge; also the diagrams involving gauge lines can be grouped by topology, with the type of gauge particle (A or B) only determining counting factors. The diagrams are listed in Figure 6; their contributions are

$$\beta_L(V_{\lambda,L} - V_{\lambda,C}) = -12\lambda^2 \frac{\xi}{4\pi} \text{ from } (p) + \quad (74)$$

$$-(4 + 2(1 + \tan^2 \Theta_W)^2) \frac{\xi}{4\pi} -$$

$$(2 + (1 + \tan^2 \Theta_W)^2) \alpha^2 \frac{\xi}{4\pi} \text{ from } (q) + \quad (75)$$

$$2(2 + (1 + \tan^2 \Theta_W)^2) \alpha^2 \frac{\xi}{4\pi} \text{ from } (r) + \quad (76)$$

$$-(2 + (1 + \tan^2 \Theta_W)^2) \alpha^2 \frac{\xi}{4\pi} \text{ from } (s) + \quad (77)$$

$$(6 + 2 \tan^2 \Theta_W) \alpha \frac{\xi}{4\pi} \lambda \text{ from } (t). \quad (78)$$

The α^2 terms all cancel, and the α term absorbs the α term in Z_Φ in the computation of $\delta\lambda_L$. The Landau gauge value could have been derived by inserting m^2 in the propagators of the ‘‘tadpole’’ contributions to the scalar self-energy and finding the $O(m^2)$ term, or equivalently by expanding the (tadpole) one loop contribution to the Landau gauge effective potential to a sufficient power in m , as discussed in Appendix A.

Seven diagrams contribute to the scalar- A field 3 point vertex. Again, they can be grouped by topology; they are presented in Figure 7. Their contributions are

$$\beta_L(V_{A,L} - V_{A,C}) = \left(\frac{5}{3} + \tan^2 \Theta_W \right) \left(-\frac{1}{3} - \frac{\alpha}{6} \right) \frac{\Sigma}{4\pi} \text{ from } (u) + \quad (79)$$

$$\left(1 + \tan^2 \Theta_W \right) \left(-3 \frac{\xi}{4\pi} + \frac{1}{6} \frac{\Sigma}{4\pi} + \frac{\alpha}{3} \frac{\Sigma}{4\pi} \right) \text{ from } (v) + \quad (80)$$

$$\left(-1 + \tan^2 \Theta_W \right) \left(\alpha \frac{\xi}{4\pi} - \frac{\alpha}{6} \frac{\Sigma}{4\pi} \right) \text{ from } (w) + \quad (81)$$

$$\left(3\alpha \frac{\xi}{4\pi} - \frac{\alpha}{6} \frac{\Sigma}{4\pi} \right) \text{ from } (x). \quad (82)$$

When using this result to get Z_A one must remember that the A field self-energy was only evaluated at $\alpha = 1$; note that there is a nonzero α dependence in $V_A + \pi_\Phi$, and hence also in π_A .

The diagrams contributing to V_B are the same as (u) through (w), but with A and B lines switched. The contributions are

$$\beta_L(V_{B,L} - V_{B,C}) = (3 + \tan^2 \Theta_W) \left(-\frac{1}{3} - \frac{\alpha}{6} \right) \frac{\Sigma}{4\pi} \text{ from } (u) + \quad (83)$$

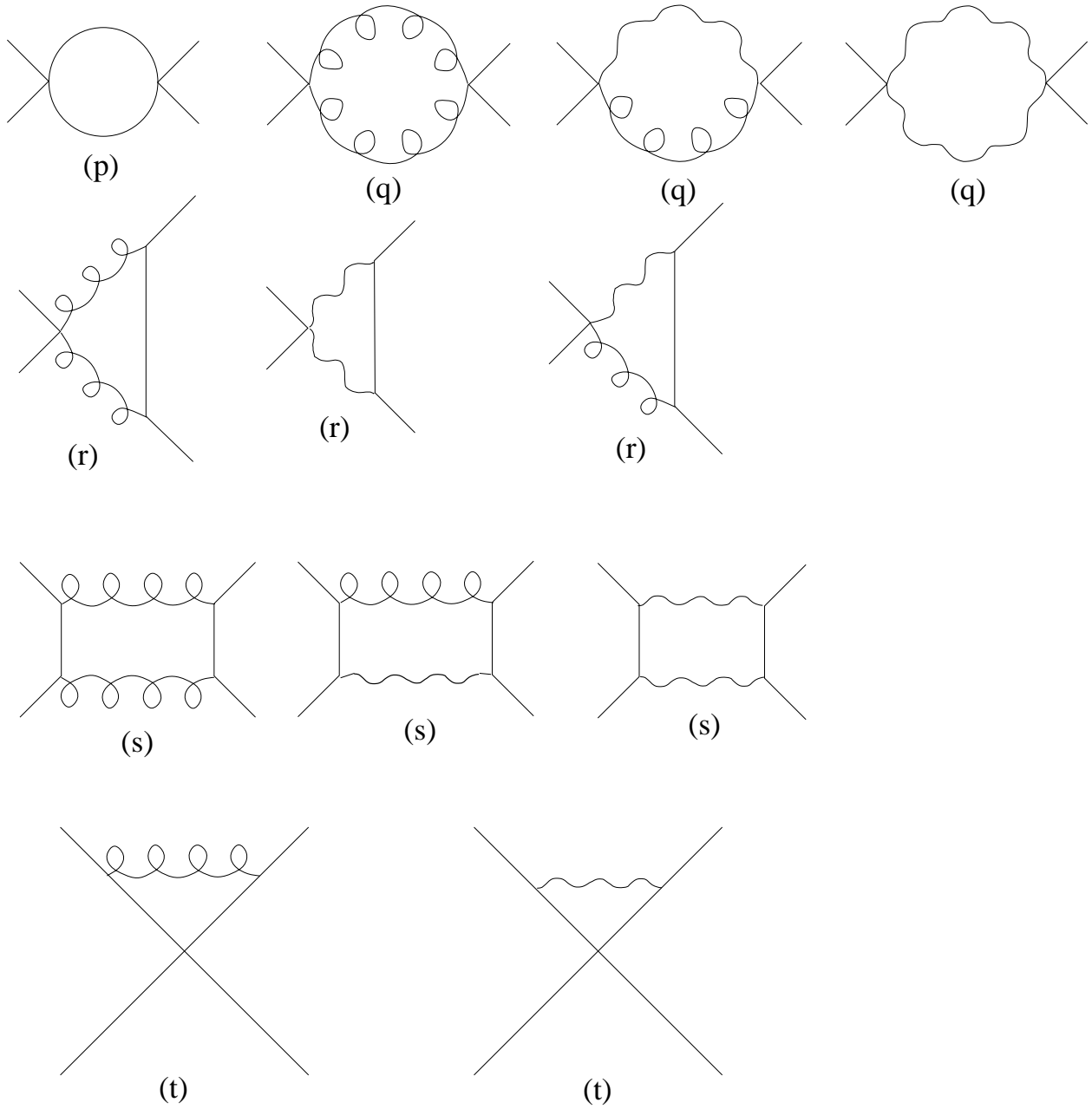


Figure 6: Contributions to the scalar 4-point function, which correct λ_L . All but (p) and (q) vanish in Landau gauge. The curly lines are SU(2) gauge propagators, the wiggly lines are U(1) gauge propagators.

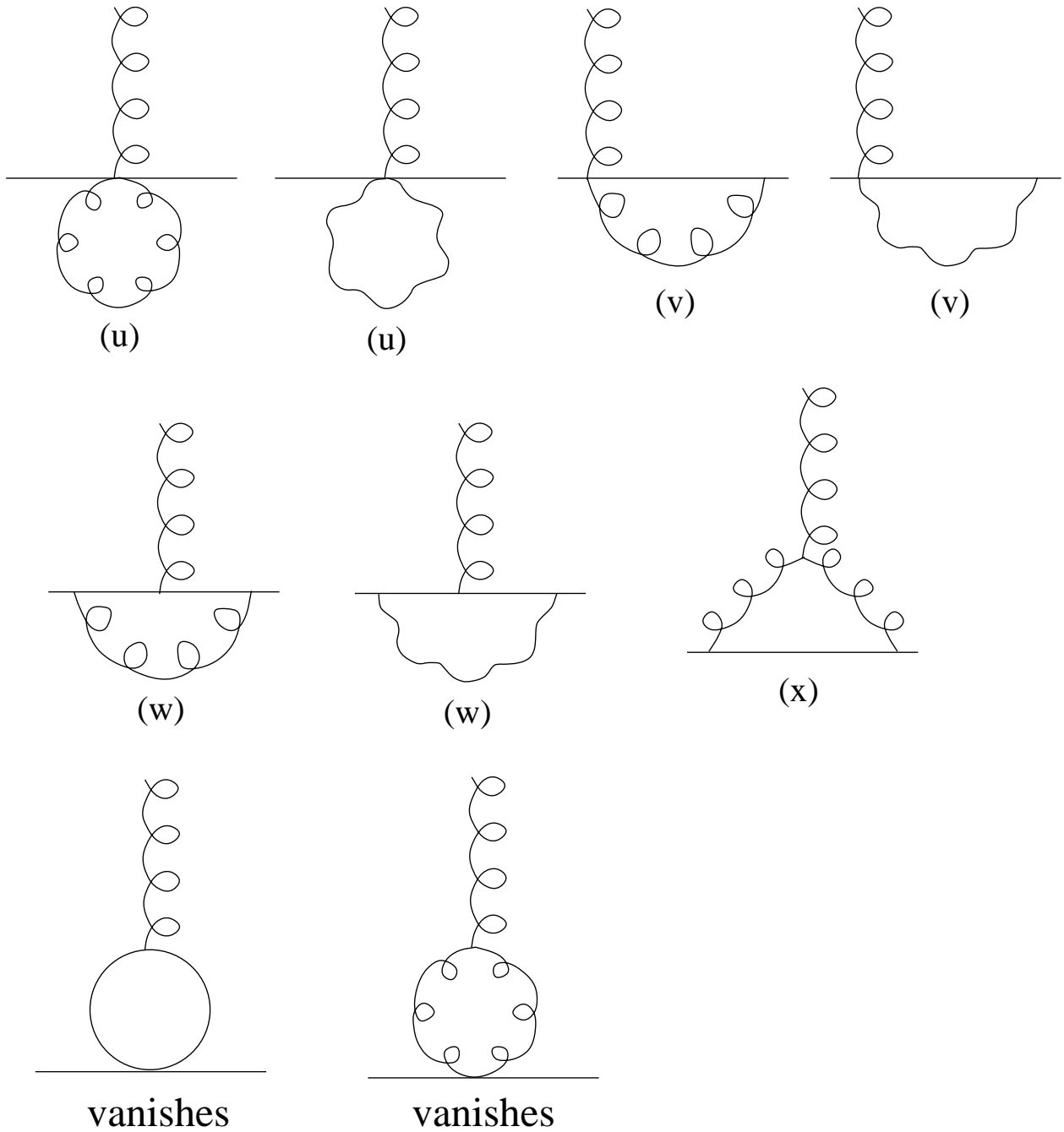


Figure 7: Contributions to the SU(2) Higgs vertex. The wiggly lines are U(1) propagators, the curly ones are SU(2) propagators, the straight ones are scalar propagators. The last two diagrams vanish on integration over the loop momenta.

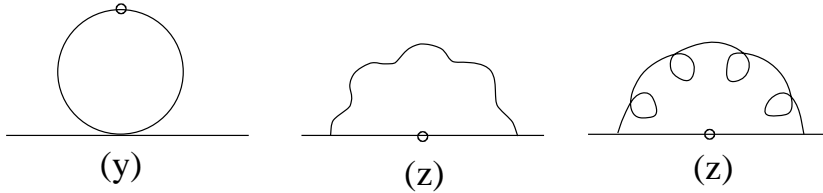


Figure 8: Contributions to the Φ^2 operator renormalization. The dots are Φ^2 operators, the plain lines are scalar propagators, the curly line is the SU(2) propagator, and the wiggly line is the U(1) propagator. The diagrams with gauge particles automatically vanish (at zero momentum) in Landau gauge.

$$(3 + \tan^2 \Theta_W) \left(-3 \frac{\xi}{4\pi} + \frac{1}{6} \frac{\Sigma}{4\pi} + \frac{\alpha}{3} \frac{\Sigma}{4\pi} \right) \quad \text{from } (v) \quad + \quad (84)$$

$$(3 + \tan^2 \Theta_W) \left(\alpha \frac{\xi}{4\pi} - \frac{\alpha}{6} \frac{\Sigma}{4\pi} \right) \quad \text{from } (w). \quad (85)$$

The total is precisely minus the total $O(p^2)$ contribution to the Higgs self-energy; hence V_B and Z_Φ cancel in the evaluation of Z_B and only π_B contributes. The same thing happens in the renormalization of continuum, 4 dimensional U(1) gauge theory.

Finally, there are three contributions to the multiplicative renormalization of the Φ^2 operator insertion, listed in Figure 8. The contributions to L_Φ are

$$\beta_L(L_{\Phi,L} - L_{\Phi,C}) = -6\lambda \frac{\xi}{4\pi} \quad \text{from } (y) \quad + \quad (86)$$

$$\alpha \left(3 + \tan^2 \Theta_W \right) \frac{\xi}{4\pi} \quad \text{from } (z), \quad (87)$$

which will cancel the α dependence in Z_Φ when one forms the gauge invariant combination $Z_\Phi Z_{OP}^{-1}$.

This concludes the evaluation of the relevant diagrams.

4 Conclusion

We have argued that the substantial linear in a corrections arising in lattice Monte-Carlo investigations of the strength of the electroweak phase transition arise from the difference between ultraviolet screening of couplings and wave functions in the continuum and lattice theories, and can be cured either with an $O(a)$ shift in the relation between the continuum and lattice couplings and wave functions or equivalently with an $O(a)$ shift in the interpretation of lattice data (the values of λ and β_L used and the jumps in order parameters).

To test the technique, we re-examine existing data, the infinite volume extrapolations of the jump in the order parameter $\beta^2 \phi^2$ for $m_H^* = 60\text{GeV}$ ($\lambda_L = 0.258$) extracted from Figure 14 of [6]. We applied $O(a)$ corrections to the data using Eqs. (25)–(27)³. We plot

³There is an $O(a^2)$ ambiguity involved in solving these equations—should one compute Z_A etc. using the uncorrected or corrected couplings? We used the corrected couplings, which means that the expressions had to be solved iteratively.

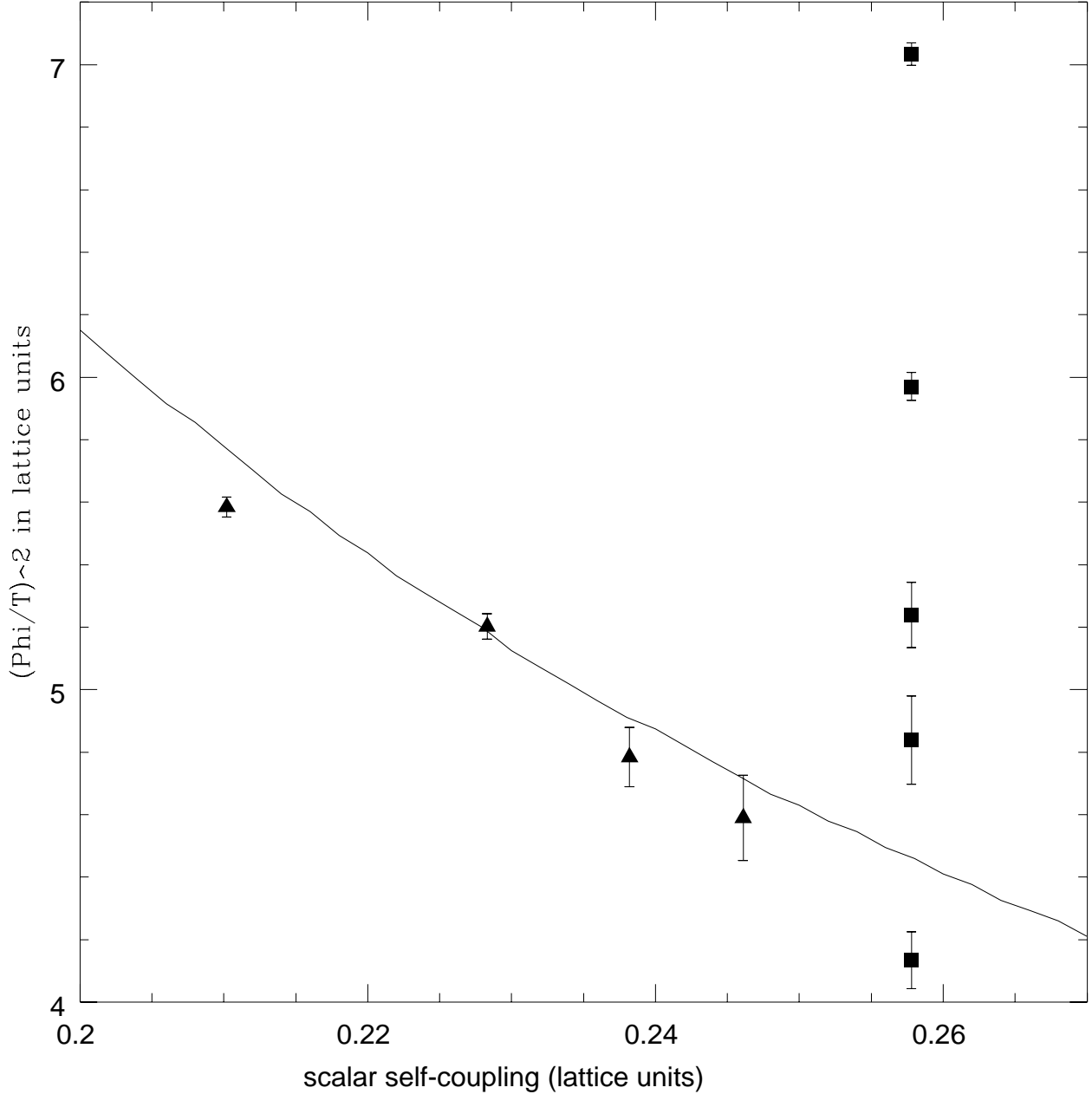


Figure 9: Jump in the order parameter as a function of scalar self-coupling, before $O(a)$ corrections (squares) and after $O(a)$ corrections (triangles). The horizontal axis is λ_L and the vertical axis is $\beta_L^2 \Phi^2$, so both are in the lattice units used here. The bottom uncorrected point is the linear extrapolation of the others, and the line is the 2 loop perturbative value. About half of the $O(a)$ errors in the original data come from the normalization of ϕ^2 and about half come from the shift in the value of λ ; after correction the data tell a consistent story and fall quite close to the two loop perturbation theory line. (The point at the smallest value of λ_L is for $\beta_L = 5$ before improvement; here $O(a^2)$ errors may be nonnegligible.)

the uncorrected and corrected jumps in the order parameter in Figure 9, which also shows the two loop perturbative value as a function of λ . The corrected data all lie quite close to the perturbative value and tell a consistent story, while the unimproved points demand a worryingly large extrapolation.

One could also correct computed surface tensions, by replacing the naive values of β_L and λ with the corrected versions in those calculations. To remove $O(a)$ errors from the calculation of other order parameters, such as the string bit or the Wilson loop, one must still compute the $O(a)$ corrections to these quantities.

So far we have said nothing about removing $O(a^2)$ errors. These arise not only from the finite renormalization of the bare couplings and wave functions, but from tree level nonrenormalizable operators. These operators modify the infrared behavior of the theory at $O(a^2)$; for instance, in Appendix A we see how high dimension derivative corrections lead at one loop to an $O(a^2)$ ϕ^5 term in the effective potential. To remove them one should start out with an “improved” action [13], rather than the minimal Wilson action we discuss here. Unfortunately the ultraviolet effects computed here will be different in such an improved action and must be recomputed.

This still leaves out the $O(a^2)$ corrections to couplings and wave functions which arise from two loop graphs. Directly computing these would involve 205 two loop diagrams for SU(2) Higgs theory, ⁴ and even more if the U(1) factor is included. It is clearly impractical to attempt this renormalization. However, one can absorb the great majority of the $O(a^2)$ corrections to wave functions and couplings in a very economical fashion, by using the tadpole improvement scheme. First, the action is tadpole improved by the technique developed by Lepage and Mackenzie [12], thereby correcting most of the loop contributions to the wave functions and couplings, at every order. Then $O(a)$ corrections to the wave functions and couplings are applied, to compensate for the difference between the full $O(a)$ corrections and those $O(a)$ corrections which the tadpole scheme will have already made. This removes all $O(a)$ errors and most $O(a^2)$ and higher order errors.

Note finally that while removing all $O(a^2)$ errors may be impossible in practice, removing all $O(a^3)$ errors is probably impossible even in principle, because there are $O(a^2)$ corrections to the ultraviolet propagators, brought about by their couplings to infrared nonperturbative physics, which are not computable and which propagate via the one loop UV corrections discussed here into $O(a^3)$ errors in the infrared wave functions and propagators. However, from a pragmatic point of view, since the dimensional reduction program itself has a limited accuracy, and since it is quite easy in practice to drive $O(a^3)$ corrections below the 1% level, this is not of practical importance.

A Integrals and Identities

In this appendix we expand the tadpole integral in powers of mass, evaluating two of the resulting integrals numerically. Then we derive a number of identities which relate all other

⁴in Landau gauge, where most of the scalar four point vertex corrections vanish automatically, there are 17 diagrams contributing to this vertex, 31 diagrams contributing to the scalar self-energy, 35 diagrams contributing to the Φ^2 operator correction, 50 diagrams contributing to the gauge self-energy, and 72 non-vanishing diagrams contributing to the gauge-scalar vertex. In a general gauge there are even more.

integrals needed in this paper to these two.

The basic integral encountered in finding the effective potential to one loop in the lattice regulation with the minimal (Wilson) action is [3]

$$aI(m) = \int_{[-\pi, \pi]^3} \frac{d^3k}{(2\pi)^3} \frac{1}{\tilde{k}^2 + (am)^2}, \quad (88)$$

where, as in the text, $\tilde{k}_i = 2 \sin(k_i/2)$ and $\tilde{k}^2 = \sum_{i=1,2,3} 4 \sin^2(k_i/2)$. Also, the $d^3k/(2\pi)^3$ will be assumed in all integrals in the remainder of the section for notational simplicity.

The integral is well behaved about $k = 0$ and so to lowest order in $am \ll 1$ it is

$$\int_{[-\pi, \pi]^3} \frac{1}{\tilde{k}^2} = \frac{\Sigma}{4\pi}, \quad \Sigma = 3.175911536. \quad (89)$$

The notation is borrowed from Farakos et. al. [3], who found an analytic expression (although the value presented above is the result of an accurate numerical integration). This gives the (divergent) mass squared correction.

Adding and subtracting this integral, we get

$$aI(m) = \frac{\Sigma}{4\pi} - \int_{[-\pi, \pi]^3} \frac{(am)^2}{\tilde{k}^2(\tilde{k}^2 + (am)^2)}. \quad (90)$$

The second integral is infrared dominated, and it is best to add and subtract the analogous continuum integral, which can be performed;

$$\int_{[-\pi, \pi]^3} \frac{(am)^2}{\tilde{k}^2(\tilde{k}^2 + (am)^2)} = \int_{\mathbb{R}^3} \frac{(am)^2}{k^2(k^2 + (am)^2)} + \quad (91)$$

$$\int_{[-\pi, \pi]^3} \left(\frac{(am)^2}{\tilde{k}^2(\tilde{k}^2 + (am)^2)} - \frac{(am)^2}{k^2(k^2 + (am)^2)} \right) -$$

$$\int_{\mathbb{R}^3 - [-\pi, \pi]^3} \frac{(am)^2}{k^2(k^2 + (am)^2)},$$

$$\int_{\mathbb{R}^3} \frac{(am)^2}{k^2(k^2 + (am)^2)} = \frac{am}{4\pi}. \quad (92)$$

This gives the famous negative cubic term in the effective potential, and leaves a remainder which vanishes as $(am)^2$.

Because $k^2 - \tilde{k}^2 = O(k^4)$ at small k , the remaining terms are well behaved about $k = 0$, and we can again extract the dominant behavior by adding and subtracting the values at $am = 0$:

$$\int_{[-\pi, \pi]^3} \left(\frac{(am)^2}{\tilde{k}^2(\tilde{k}^2 + (am)^2)} - \frac{(am)^2}{k^2(k^2 + (am)^2)} \right) - \int_{\mathbb{R}^3 - [-\pi, \pi]^3} \frac{(am)^2}{k^2(k^2 + (am)^2)} =$$

$$(am)^2 \left[\int_{[-\pi, \pi]^3} \left(\frac{1}{(\tilde{k}^2)^2} - \frac{1}{k^4} \right) - \int_{\mathbb{R}^3 - [-\pi, \pi]^3} \frac{1}{k^4} \right] - (am)^4 \times \quad (93)$$

$$\left[\int_{[-\pi, \pi]^3} \left(\frac{1}{(\tilde{k}^2)^2(\tilde{k}^2 + (am)^2)} - \frac{1}{k^4(k^2 + (am)^2)} \right) - \int_{\mathbb{R}^3 - [-\pi, \pi]^3} \frac{1}{k^4(k^2 + (am)^2)} \right] \quad (94)$$

Following the notation of [3] we denote the first integral as

$$\left[\int_{[-\pi, \pi]^3} \left(\frac{1}{(\tilde{k}^2)^2} - \frac{1}{k^4} \right) - \int_{\mathbb{R}^3 - [-\pi, \pi]^3} \frac{1}{k^4} \right] = \frac{\xi}{4\pi}. \quad (95)$$

To evaluate it numerically we reduce the second integral to a single integral over a polar angle,

$$\int_{\mathbb{R}^3 - [-\pi, \pi]^3} \frac{1}{k^4} = \frac{1}{4\pi^3} + \frac{1}{\pi^4} \int_0^{\pi/4} \cos(\theta) \arctan(\cos(\theta)) d\theta = 0.0134035706 \quad (96)$$

and perform the first numerically, directly. The result is $\xi = 0.152859325$. This enters the coefficient of an $O(a)$ contribution to the effective potential which behaves as ϕ^4 ; summing over species, one can derive V_λ in Landau gauge.

Finally, Eq. (94) is infrared dominated and $O((am)^3)$, because $k^2 - \tilde{k}^2$ is order k^4 at small k ; had it been order k^6 then the infrared would be well behaved in this integral. To extract this infrared $O((am)^3)$ piece one should expand \tilde{k}^2 to $O(k^4)$,

$$\sum_i 4 \sin(k_i/2) = \sum_i k_i^2 - \frac{1}{12} \sum_i k_i^4, \quad (97)$$

from which it follows that the contribution –Eq. (94) to the effective potential is approximately

$$\begin{aligned} & (am)^4 \int_{\mathbb{R}^3} \sum_i k_i^4 \left(\frac{2k^2 + (am)^2}{k^4(k^2 + (am)^2)^2} - \frac{2}{k^6} \right) \\ &= \frac{(am)^3}{32\pi}. \end{aligned} \quad (98)$$

This generates an $O(a^2)$ term in the effective potential of form ϕ^5 and is caused by the (tree level) nonrenormalizable derivative terms in the action arising from the choice of lattice regulation. Had the expansion of \tilde{k}^2 been free of the $O(k^4)$ part, no such term would appear and the first one loop effect beyond the $O(a)$ correction to λ would be an $O(a^3)$ induced nonrenormalizable ϕ^6 term. (Of course, there would still be $O(a^2)$ corrections to λ arising at two loops.)

Several other integrals arise in the calculations in the text, but a number of identities relate them all to the two (numerical) integrals, Eq. (89) and Eq. (95). Some of these identities involve trigonometric manipulations of numerators, for instance using $\cos^2(k_i/2) = 1 - \tilde{k}_i^2/4$ and $\cos(k_i) = 1 - \tilde{k}_i^2/2$; we will not bother to list these here. Some use cubic invariance;

$$\int_{[-\pi, \pi]^3} \frac{\tilde{k}_1^2}{(\tilde{k}^2)^2} = \frac{1}{3} \int_{[-\pi, \pi]^3} \frac{\tilde{k}_1^2 + \tilde{k}_2^2 + \tilde{k}_3^2}{(\tilde{k}^2)^2} = \frac{1}{3} \int_{[-\pi, \pi]^3} \frac{1}{\tilde{k}^2} = \frac{1}{3} \frac{\Sigma}{4\pi}. \quad (99)$$

Similarly,

$$\int_{[-\pi, \pi]^3} \frac{\tilde{k}_1^2}{\tilde{k}^2} = \frac{1}{3} \quad (100)$$

and

$$\int_{[-\pi, \pi]^3} \frac{\tilde{k}_1^2}{(\tilde{k}^2)^3} - \text{continuum version} = \frac{1}{3} \frac{\xi}{4\pi}. \quad (101)$$

Here “- continuum version” means that k_1^2/k^6 should be subtracted from the integrand and the integral of k_1^2/k^6 outside the first Brillion zone should also be subtracted. In what follows the meaning will be analogous.

Cubic invariance cannot be used to evaluate the integral over $\tilde{k}_i^4/(\tilde{k}^2)^3$. To do so we must take advantage of the periodicity of the integrand on 2π shifts in any k_i . For ϵ an infinitesimal, the periodicity of \tilde{k}_1^2 ensures that

$$\int_{[-\pi, \pi]^3} \frac{1}{\tilde{k}^2} = \int_{[-\pi, \pi]^3} \frac{1}{(2 \sin^2((k_1 + \epsilon)/2))^2 + \tilde{k}_2^2 + \tilde{k}_3^2}. \quad (102)$$

Now, excising a small neighborhood about the origin to avoid the singularity there, one can expand in ϵ . At order ϵ^2 , one finds after some work that

$$0 = \int_{[-\pi, \pi]^3 - \text{excision}} \left(-\frac{1}{(\tilde{k}^2)^2} + \frac{1}{2} \frac{\tilde{k}_1^2}{(\tilde{k}^2)^3} + 4 \frac{\tilde{k}_1^2}{(\tilde{k}^2)^3} - \frac{\tilde{k}_1^4}{(\tilde{k}^2)^3} \right) + \text{surface term}, \quad (103)$$

where the surface term arises on the boundary of the excised region. It cancels the linear infrared divergence occurring from the two terms with $O(1/k^4)$ infrared behavior, so what remains is the difference between these terms and their continuum analogs, eg $\int 1/(\tilde{k}^2)^2$ becomes Eq. (95). Using the previous integrals and identities we can integrate all but the last term, so we find that

$$\int_{[-\pi, \pi]^3} \frac{\tilde{k}_1^4}{(\tilde{k}^2)^3} = \frac{1}{6} \frac{\Sigma}{4\pi} + \frac{1}{3} \frac{\xi}{4\pi}. \quad (104)$$

Because $\tilde{k}_1^2 + \tilde{k}_2^2 + \tilde{k}_3^2 = \tilde{k}^2$, it follows from this integral, Eq. (99), and cubic invariance that

$$\int_{[-\pi, \pi]^3} \frac{\tilde{k}_1^2 \tilde{k}_2^2}{(\tilde{k}^2)^3} = \frac{1}{12} \frac{\Sigma}{4\pi} - \frac{1}{6} \frac{\xi}{4\pi}. \quad (105)$$

Repeating the above technique, but starting with the integral over $\ln(\tilde{k}^2)$ rather than $1/\tilde{k}^2$, one finds that

$$0 = \int_{[-\pi, \pi]^3} \frac{-2\tilde{k}^2 + \tilde{k}^2 \tilde{k}_1^2 + 4\tilde{k}_1^2 - \tilde{k}_1^4}{(\tilde{k}^2)^2}, \quad (106)$$

or

$$\int_{[-\pi, \pi]^3} \frac{\tilde{k}_1^4}{(\tilde{k}^2)^2} = \frac{1}{3} - \frac{2}{3} \frac{\Sigma}{4\pi}, \quad (107)$$

and hence also

$$\int_{[-\pi, \pi]^3} \frac{\tilde{k}_1^2 \tilde{k}_2^2}{(\tilde{k}^2)^2} = \frac{1}{3} \frac{\Sigma}{4\pi}. \quad (108)$$

Continuing the expansion to fourth order in ϵ , and using the previously derived identities, one obtains after considerable algebra that

$$\int_{[-\pi,\pi]^3} \frac{\tilde{k}_1^4(1 - \tilde{k}_1^2/4)^2}{(\tilde{k}^2)^4} - \text{continuum version} - \int_{[-\pi,\pi]^3} \frac{\tilde{k}_1^2(1 - \tilde{k}_1^2/2)(1 - \tilde{k}_1^2/4)}{(\tilde{k}^2)^3} - \text{continuum version} = -\frac{1}{48} + \frac{1}{8} \frac{\Sigma}{4\pi} - \frac{1}{8} \frac{\xi}{4\pi}. \quad (109)$$

Shifting the k_2 integral by δ , the condition that the $O(\epsilon^2\delta^2)$ term should vanish gives that

$$3 \int_{[-\pi,\pi]^3} \frac{\tilde{k}_1^2\tilde{k}_2^2(1 - \tilde{k}_1^2/4)(1 - \tilde{k}_2^2/4)}{(\tilde{k}^2)^4} - \text{continuum version} - \int_{[-\pi,\pi]^3} \frac{\tilde{k}_1^2(1 - \tilde{k}_2^2/2)(1 - \tilde{k}_1^2/4)}{(\tilde{k}^2)^3} - \text{continuum version} = \frac{1}{32} \frac{\Sigma}{4\pi} - \frac{1}{8} \frac{\xi}{4\pi}. \quad (110)$$

By shifting k_1 by ϵ in the integral

$$\int_{[-\pi,\pi]^3} \frac{\tilde{k}_2^2}{\tilde{k}^2} \quad (111)$$

and expanding to second order in ϵ , one finds using Eq. (108) that

$$\int_{[-\pi,\pi]^3} \frac{\tilde{k}_1^4\tilde{k}_2^2}{(\tilde{k}^2)^3} = \frac{1}{6} \frac{\Sigma}{4\pi} - \frac{2}{3} \frac{\xi}{4\pi}, \quad (112)$$

and hence

$$\int_{[-\pi,\pi]^3} \frac{\tilde{k}_1^6}{(\tilde{k}^2)^3} = \frac{1}{3} - \frac{\Sigma}{4\pi} + \frac{4}{3} \frac{\xi}{4\pi}, \quad (113)$$

by applying the same technique used to get Eq. (105) and using Eq. (107). With these integrals we can derive that

$$\int_{[-\pi,\pi]^3} \frac{\tilde{k}_1^2(1 - \tilde{k}_1^2/2)(1 - \tilde{k}_1^2/4)}{(\tilde{k}^2)^3} - \text{continuum version} = \frac{1}{24} - \frac{1}{4} \frac{\Sigma}{4\pi} + \frac{1}{4} \frac{\xi}{4\pi}, \quad (114)$$

and

$$\int_{[-\pi,\pi]^3} \frac{\tilde{k}_1^2(1 - \tilde{k}_2^2/2)(1 - \tilde{k}_1^2/4)}{(\tilde{k}^2)^3} - \text{continuum version} = -\frac{1}{16} \frac{\Sigma}{4\pi} + \frac{1}{4} \frac{\xi}{4\pi}. \quad (115)$$

Hence we know the value of each integral in Eqs. (109) and (110) separately.

No other identities are needed for to complete the 1 loop renormalization.

The figure shows three Feynman diagrams and their corresponding mathematical expressions:

- Top diagram:** A four-point vertex with four external lines labeled p,i , q,j , r,k , and s,l . The lines are wavy. The corresponding expression is:

$$\frac{1}{2} \sum_{m,n} (\mathbf{p}_m \delta_{in} - \mathbf{p}_n \delta_{im}) (\mathbf{q}_m \delta_{jn} - \mathbf{q}_n \delta_{jm}) (\mathbf{r}_m \delta_{kn} - \mathbf{r}_n \delta_{km}) (\mathbf{s}_m \delta_{ln} - \mathbf{s}_n \delta_{lm})$$
- Middle diagram:** A three-point vertex with two external lines labeled p,a and q,b (horizontal, straight) and one external line labeled r,i,A (vertical, wavy). The corresponding expression is:

$$-(i \tau^A)_{ab} i \widetilde{\mathbf{p}_i - \mathbf{q}_i} \delta(\mathbf{p} + \mathbf{q} + \mathbf{r})$$
- Bottom diagram:** A three-point vertex with two external lines labeled p,a and q,b (horizontal, straight) and one external line labeled r,i (vertical, wavy). The corresponding expression is:

$$-(i)_{ab} i \widetilde{\mathbf{p}_i - \mathbf{q}_i} \delta(\mathbf{p} + \mathbf{q} + \mathbf{r})$$

Figure 10: Feynman rules for the U(1) four point function and the three point gauge-Higgs couplings.

B Feynman rules

Most of the Feynman rules needed in the calculation appear in [14]; the measure insertion (diagram (h) in Section 3) is smaller by a factor of $2/3$ from the one printed there, which is for SU(3) rather than SU(2), and similarly in the four point vertex in Eq. (14.44) one must set d_{ABC} to 0 and the $(2/3)$ in front of $\delta_{AB}\delta_{BC} + \delta_{AC}\delta_{BD} + \dots$ should become 1. Our conventions for the scale and the gauge wave function mean a should be replaced by 1 and g by 2 everywhere. Also, the sign for the ghost coupling to two gauge particles is backwards there.

What remains are the scalar propagator and the vertices involving the scalar. The propagator, in the ultraviolet where m is negligible, is just δ_{ab}/p^2 . The 4-point vertex is

$$-2\lambda(\delta_{ab}\delta_{cd} + \delta_{ac}\delta_{bd} + \delta_{ad}\delta_{bc}) \quad (116)$$

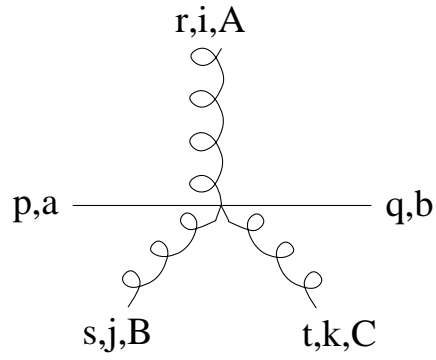
where a, b, c, d are the species types of the incoming lines. The vertices involving gauge particles, and the pure U(1) four point vertex, are given in Figures 10 to 12. The notation is that $(i)_{ab}$ means the action of i on the species type, eg species type 1 becomes type 2 and type 2 becomes $-$ type 1, etc. Any i by itself is the imaginary number which arises when one Fourier transforms an odd function. The vertices in Figure 12 do not have continuum analogs. Their role in generating extra tadpole diagrams is quite important on the lattice; for instance they dominate the corrections V_B to the U(1)- Higgs vertex.

$$\begin{array}{c}
 r,i,A \\
 \text{---} \\
 p,a \text{ ---} \text{---} q,b \\
 \text{---} \\
 s,j,B
 \end{array}
 \quad -2 \delta_{AB} \delta_{ij} \delta_{ab} \cos\left(\frac{p_i - q_i}{2}\right) \delta(p+q+r+s)$$

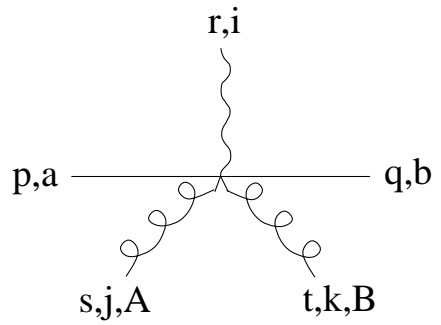
$$\begin{array}{c}
 r,i \\
 \text{---} \\
 p,a \text{ ---} \text{---} q,b \\
 \text{---} \\
 s,j
 \end{array}
 \quad -2 \delta_{ab} \delta_{ij} \cos\left(\frac{p_i - q_i}{2}\right) \delta(p+q+r+s)$$

$$\begin{array}{c}
 r,i \\
 \text{---} \\
 p,a \text{ ---} \text{---} q,b \\
 \text{---} \\
 s,j,B
 \end{array}
 \quad 2 (i)_{ac} (i \tau^A)_{cb} \cos\left(\frac{p_i - q_i}{2}\right) \delta(p+q+r+s)$$

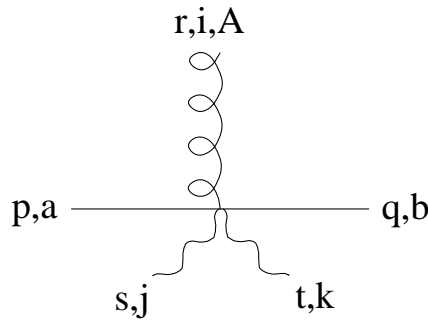
Figure 11: Feynman rules for the four point gauge-Higgs couplings.



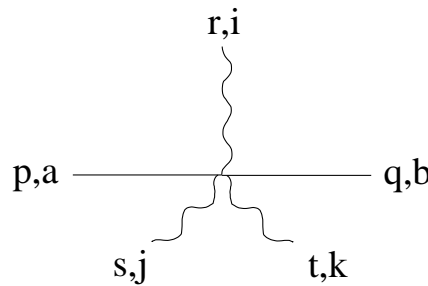
$$\frac{1}{3} (\delta_{AB} \delta_{CD} + \delta_{AC} \delta_{BD} + \delta_{AD} \delta_{BC}) \delta_{ijk} (i\tau^D)_{ab} i \widetilde{p_i - q_i} \delta(p+q+r+s+t)$$



$$\delta_{AB} \delta_{ijk} (i)_{ab} i \widetilde{p_i - q_i} \delta(p+q+r+s+t)$$



$$(i\tau^A)_{ab} \delta_{ijk} i \widetilde{p_i - q_i} \delta(p+q+r+s+t)$$



$$(i)_{ab} \delta_{ijk} i \widetilde{p_i - q_i} \delta(p+q+r+s+t)$$

Figure 12: Feynman rules for the five point gauge-Higgs couplings.

C Results in other theories

Here we present results for the renormalization of the abelian Higgs model with N scalars, and for $SU(2) \times U(1)$ theory with adjoint scalars (the Weinberg-Salaam model after dimensional reduction but before integrating out heavy modes).

The action of the 3-D abelian Higgs model on a lattice is

$$\sum_x \left[Z_B \sum_{i < j} (1 - \text{Re } p_{ij}) + Z_\Phi \sum_{b=1}^N \sum_i \left(\Phi_b^2(x) - \Phi_{ab}(x) u_{iac}(x) \Phi_{cb}(x+i) \right) + Z_\Phi \frac{m_{HL}^2}{2} \left(\sum_b \Phi_b^2 \right) + Z_\Phi^2 \frac{\lambda_L}{4} \left(\sum_b \Phi_b^2 \right)^2 \right]. \quad (117)$$

Here a and c are indicies over the real and imaginary part, which are implicitly summed over when Φ^2 appears, and b is an index over the N scalar species, which are assumed to have the same mass squared and an $SU(N)$ symmetric quartic interaction. The finite a renormalization only involves diagrams computed already in the text; the results are

$$\beta_L \delta \lambda_L = \frac{1}{3} \frac{\Sigma}{4\pi} + \left(6\lambda_L - (10 + 2N)\lambda_L^2 - 2 \right) \frac{\xi}{4\pi}, \quad (118)$$

$$\beta_L (Z_B - 1) = \frac{1}{3} + N \left(\frac{1}{8} \frac{\Sigma}{4\pi} - \frac{1}{2} \frac{\xi}{4\pi} \right), \quad (119)$$

$$\beta_L \delta m_{HL}^2 = (2 + (4 + 2N)\lambda_L) \frac{\Sigma}{4\pi}, \quad (120)$$

$$\beta_L (Z_\Phi Z_{OP}^{-1} - 1) = (3 - (4 + 2N)\lambda_L) \frac{\xi}{4\pi} + \frac{1}{6} \frac{\Sigma}{4\pi}. \quad (121)$$

Next we consider $SU(2) \times U(1)$ theory, with an adjoint $SU(2)$ scalar A_0 and an adjoint $U(1)$ scalar B_0 . If one is interested in very high precision calculations of the electroweak phase transition strength one must include these, because the integration over these fields (the so called heavy modes) is lower precision than the integration over the nonzero Matsubara frequencies (the superheavy modes).

The integration over the zero Matsubara frequencies generates mass terms for these modes. Interaction terms already exist at tree level, and new ones are generated at one loop in the dimensional reduction. The new mass terms will be denoted m_A^2 and m_B^2 , and the new interaction terms in the Lagrangian are

$$\frac{\lambda_A}{4} (A_0^2)^2 + \frac{\lambda_B}{4} (B_0^2)^2 + \frac{h_A}{4} \Phi^2 A_0^2 + \frac{h_B}{4} \Phi^2 B_0^2 + \frac{h_{AB}}{4} A_0^2 B_0^2 + \frac{h'}{2} B_0 \Phi_a (-A_0 \cdot \tau)_{ab} \Phi_b. \quad (122)$$

In the minimal standard model, at lowest order in α_W , the bare values for the new couplings, in lattice units, are [4]

$$\lambda_{AL} = 0, \quad (123)$$

$$\lambda_{BL} = 0, \quad (124)$$

$$h_{AL} = 2, \quad (125)$$

$$h_{BL} = 2 \tan^2 \Theta_W, \quad (126)$$

$$h_{ABL} = 0, \quad (127)$$

$$h'_L = 2 \tan \Theta_W, \quad (128)$$

but in what follows we will treat the general problem in which their values are arbitrary. Computing the $O(a)$ renormalizations involves no topologically new diagrams, only combinatorics. The couplings and wave functions presented in Section 2 are modified by

$$\frac{\Sigma}{4\pi} - 4\frac{\xi}{4\pi} \quad \text{added to} \quad \beta_L(Z_A - 1), \quad (129)$$

$$-\frac{3}{4}h_{AL}^2 - \frac{1}{4}h_{BL}^2 - \frac{1}{2}h_L'^2 \quad \text{added to} \quad \beta_L\delta\lambda_L, \quad (130)$$

$$\frac{3}{2}h_{AL} + \frac{1}{2}h_{BL} \quad \text{added to} \quad \beta_L\delta m_{HL}^2. \quad (131)$$

The corrections to Z_B and Z_Φ vanish.

We denote the new wave function corrections as Z_{A0} and Z_{B0} ; the notations for the coupling corrections are obvious. The new couplings and wave functions renormalize by

$$\beta_L(Z_{A0} - 1) = 24\frac{\xi}{4\pi} + \frac{4}{3}\frac{\Sigma}{4\pi} - 5\lambda_{AL}\frac{\xi}{4\pi}, \quad (132)$$

$$\beta_L(Z_{B0} - 1) = -3\lambda_{BL}\frac{\xi}{4\pi}, \quad (133)$$

$$\beta_L\delta m_{AL}^2 = \left(16 + 5\lambda_L + 2h_{AL} + \frac{1}{2}h_{ABL}\right)\frac{\Sigma}{4\pi}, \quad (134)$$

$$\beta_L\delta m_{BL}^2 = \left(3\lambda_{BL} + 2h_{BL} + \frac{3}{2}h_{ABL}\right)\frac{\Sigma}{4\pi}, \quad (135)$$

$$\beta_L\delta\lambda_{AL} = -\left(32 + 11\lambda_{AL}^2 + h_{AL}^2 + \frac{1}{4}h_{ABL}^2\right)\frac{\xi}{4\pi} + \lambda_{AL}\left(48\frac{\xi}{4\pi} + \frac{8}{3}\frac{\Sigma}{4\pi}\right), \quad (136)$$

$$\beta_L\delta\lambda_{BL} = -\left(10\lambda_{BL}^2 + h_{BL}^2 + \frac{3}{4}h_{ABL}^2\right)\frac{\xi}{4\pi}, \quad (137)$$

$$\begin{aligned} \beta_L\delta h_{AL} = & -\left(8 + 6\lambda_L h_{AL} + 5\lambda_{AL} h_{AL} + 2h_{AL}^2 + \frac{1}{2}h_{BL} h_{ABL} + 2h_L'^2\right)\frac{\xi}{4\pi} + \\ & h_{AL}\left(\left(33 + 3\tan^2\Theta_W\right)\frac{\xi}{4\pi} + \left(\frac{11}{6} + \frac{1}{6}\tan^2\Theta_W\right)\frac{\Sigma}{4\pi}\right), \end{aligned} \quad (138)$$

$$\begin{aligned} \beta_L\delta h_{BL} = & -\left(6\lambda_L h_{BL} + 3\lambda_{BL} h_{BL} + 2h_{BL}^2 + \frac{3}{2}h_{AL} h_{ABL} + 2h_L'^2\right) + \\ & h_{BL}\left(\left(9 + 3\tan^2\Theta_W\right)\frac{\xi}{4\pi} + \left(\frac{3 + \tan^2\Theta_W}{6}\right)\frac{\Sigma}{4\pi}\right), \end{aligned} \quad (139)$$

$$\begin{aligned} \beta_L\delta h_{ABL} = & -\left(5\lambda_{AL} h_{ABL} + 3\lambda_{BL} h_{ABL} + 2h_{ABL}^2 + 2h_{AL} h_{BL} + 2h_L'^2\right) + \\ & h_{ABL}\left(24\frac{\xi}{4\pi} + \frac{4}{3}\frac{\Sigma}{4\pi}\right), \end{aligned} \quad (140)$$

$$\begin{aligned} \beta_L\delta h_L' = & h_L'\left(\left(-2\lambda_L - h_{AL} - h_{BL} - h_{ABL} + 21 + 3\tan^2\Theta_W\right)\frac{\xi}{4\pi} + \right. \\ & \left. \frac{7 + \tan^2\Theta_W}{6}\frac{\Sigma}{4\pi}\right). \end{aligned} \quad (141)$$

Here the wave functions already include corrections to make the operator insertions have their naive normalization. In fact the operator insertions will be mixed by a matrix with

$O(a)$ off diagonal terms; what we use above are the diagonal components of the matrix. The off diagonal terms would only be important if the A_0 or B_0 fields took on significant condensates at the phase transition, which they should not, because in the realistic case they should be given substantial (Debye) masses. They would also be important if we were interested in the jumps in these condensates, but this is also not of interest. We have not computed the off diagonal terms here.

References

- [1] P. Arnold and O. Espinoza, Phys. Rev. **D 47** (1993) 3546; Z. Fodor and A. Hebecker, Nucl. Phys. **B 432** (1994) 127.
- [2] K. Kajantie, K. Rummukainen, and M. Shaposhnikov, Nucl. Phys. **B 407** (1993) 356; K. Farakos, K. Kajantie, K. Rummukainen, and M. Shaposhnikov, Nucl. Phys. **B 425** (1994) 67.
- [3] K. Farakos, K. Kajantie, K. Rummukainen, and M. Shaposhnikov, Nucl. Phys. **B 442** (1995) 317.
- [4] K. Kajantie, M. Laine, K. Rummukainen, and M. Shaposhnikov, Nucl. Phys. **B 458** (1996) 90.
- [5] K. Farakos, K. Kajantie, K. Rummukainen, and M. Shaposhnikov, Phys. Lett. **B 336** (1994) 194; K. Farakos, K. Kajantie, M. Laine, K. Rummukainen, and M. Shaposhnikov, Nucl. Phys. **B** (Proc. Suppl.) **17** (1996) 705.
- [6] K. Kajantie, M. Laine, K. Rummukainen, and M. Shaposhnikov, Nucl. Phys. **B 466** (1996) 189.
- [7] K. Kajantie, M. Laine, K. Rummukainen, and M. Shaposhnikov, CERN-TH-96-126, hep-ph/9605288.
- [8] E. Ilgenfritz, J. Kripfganz, H. Perlt, and A. Schiller, Phys. Lett. **B 356** (1995) 561; M. Gurtler, E. Ilgenfritz, J. Kripfganz, H. Perlt, and A. Schiller, hep-lat/9512022; hep-lat/9605042.
- [9] F. Karsch, T. Neuhaus, A. Patkos, and J. Rank, BI-TP-96-10 (hep-lat/9603004).
- [10] O. Philipsen, M. Teper, and H. Wittig, Nucl. Phys. **B 469** (1996), 445; hep-lat/9608067.
- [11] M. Laine, Nucl. Phys. **B 451** (1995) 484.
- [12] G. P. Lepage and P. Mackenzie, Phys. Rev. **D 48** (1993) 2250.
- [13] P. Weisz, Nucl. Phys. **B 212** (1983), 1; G. Curci, P. Menotti, and G. Paffuti, Phys. Lett. **B 130** (1983), 205.
- [14] H. J. Rothe, “Lattice Gauge Theories: an Introduction” (World Scientific, Singapore, 1992).